The Astrophysical Journal, 592:504–515, 2003 July 20

BINARY BLUE METAL-POOR STARS: EVIDENCE FOR ASYMPTOTIC GIANT BRANCH MASS TRANSFER

Christopher Sneden,[1,2] George W. Preston,[2] and John J. Cowan[3]

Received 2003 February 8; accepted 2003 April 1

ABSTRACT

We present new abundance analyses of six blue metal-poor (BMP) stars with very low iron abundances ([Fe/H] < -2), based on new high-resolution echelle spectra. Three are spectroscopic binaries, and three have constant radial velocities. The chemical compositions of these two groups are very different, as the binary BMP stars have large enhancements of carbon and neutron-capture elements that are products of *s*-process nucleosynthesis. One star, CS 29497−030, has an extreme enhancement of lead, [Pb/Fe] $= +3.7$, the largest abundance in any star yet discovered. It probably also has an oxygen overabundance compared to the other BMP stars of our sample. The binary BMP stars must have attained their status via mass transfer during the asymptotic giant branch (AGB) evolutions of their companion stars, which are now unseen and most likely are compact objects. We have not found any examples of AGB mass transfer among BMP binaries with [Fe/H] > -2.

Subject headings: Galaxy: halo — nuclear reactions, nucleosynthesis, abundances — stars: abundances — stars: Population II

On-line material: color figures

1. INTRODUCTION

Many Galactic globular clusters possess a small number of so-called blue stragglers—main-sequence stars that are clearly bluer and brighter than the turnoff stars. Blue stragglers are generally believed to have formed from stellar mergers in the high-density environments of these clusters (e.g., Stryker 1993; Sills & Bailyn 1999).

Stellar collisions are less frequent in the disk and halo by many orders of magnitude, so the substantial numbers of field blue stragglers (FBSs) identified and discussed by Preston, Beers, & Shectman (1994) and Preston & Sneden (2000, hereafter PS00) must be created by the only remaining mechanism, McCrea (1964) mass transfer. Of 62 blue metal-poor (BMP) stars investigated by PS00, 2/3 are in single-lined spectroscopic binaries with orbital periods in the approximate interval $2 < P(\mathrm{days}) < 4000$. Analysis of the data indicates that half or more of the BMP stars are ordinary lower main-sequence stars that gain mass from their companions during the post–main-sequence evolution of the latter. The unseen companions are now some sort of compact white dwarf–like objects. We have argued that the remainder of the sample, including nearly all the single stars, are metal-poor stars of intermediate age. A few of the single BMP stars may be the products of merger of the small fraction of binaries (<10%) with initial periods less than ~5 days (Vilhu 1982). The intermediate-age population should also contribute its modest (~20%) share of spectroscopic binaries. Because we cannot imagine where in the Galaxy it would be possible to preserve metal-poor gas for billions of years, we suggest that these intermediate-age stars may have been captured from metal-poor dwarf galaxies like the Carina dwarf spheroidal (Smecker-Hane et al. 1994).

PS00 included determinations of Fe metallicities and abundance ratios of eight elements in most of the 62 star BMP sample, using co-added spectra of each star to increase the signal-to-noise ratio (S/N). Examples of individual and summed spectra are shown in Figure 1 of that paper. Derived stellar metallicities were found to be uniformly spread over the range $0.0 \gtrsim [\mathrm{Fe/H}] \gtrsim -2.5$. A normal halo abundance pattern was derived for stars with [Fe/H] < -0.5. That is, the vast majority of BMP stars have enhancements of α-elements: [Mg/Fe] $\approx$ [Ca/Fe] $\approx$ [Ti/Fe] $\approx +0.30 \pm 0.20$. For Fe-peak elements, [Sc/Fe] $\approx$ [Cr/Fe] $\approx 0.00 \pm 0.25$. And among neutron-capture (*n*-capture) elements, [Sr/Fe] $\sim$ [Ba/Fe] ~ 0.0 for stars with [Fe/H] > -2.0, but for lower metallicities very large star-to-star scatter was found, especially so for Ba.

PS00 made no attempt to compare abundance ratio systematics between the BMP binaries and those with no detectable radial velocity variations (hereafter called RV-constant stars). As part of an ongoing program to understand the differences in these two BMP subclasses, we gathered new high-resolution spectra of five binaries and five RV-constant stars. Three stars in each of these groups have very low metallicities, [Fe/H] ≈ -2.1. In this paper we concentrate on analyses of these six stars, concluding that significant differences exist between the abundances of carbon and the *n*-capture elements of the binaries and the RV-constant stars. We argue that mass transfer from a former asymptotic giant branch (AGB) companion star must have created the binary BMP stars that we observe now. We detect Pb in the spectrum of one of the BMP binaries and find that this star has the largest Pb abundance reported to date. In § 2 the observations are presented. In § 3 the new radial velocities are given, along with revised orbits for the binary stars. We discuss the abundance analysis in § 4 and the implications of the abundances on the formation of binary BMP stars in § 5.

[1] Department of Astronomy and McDonald Observatory, University of Texas, Austin, TX 78712; chris@verdi.as.utexas.edu.

[2] Carnegie Observatories, 813 Santa Barbara Street, Pasadena, CA 91101; gwp@ociw.edu.

[3] Department of Physics and Astronomy, University of Oklahoma, Norman, OK 73019; cowan@mail.nhn.ou.edu.

TABLE 1
BASIC DATA AND MODEL ATMOSPHERE PARAMETERS

Star	V	$(B-V)_0$	$(U-B)_0$	$V_e \sin i$	$T_{\rm eff}$	$\log g$	v_t	[Fe/H]
RV-constant Stars								
22876−042	13.1	0.35	−0.21	8	6750	4.2	2.50	−2.06
22941−012	12.5	0.28	−0.17	10	7200	4.2	2.50	−2.03
22964−214	13.7	0.35	−0.19	12	6800	4.5	2.00	−2.30
Binaries								
22956−028	13.0	0.34	−0.17	15	6900	3.9	2.00	−2.08
29497−030	12.7	0.30	−0.14	12	7050	4.2	1.75	−2.16
29509−027	12.5	0.29	−0.13	10	7050	4.2	2.00	−2.02

2. OBSERVATIONS AND REDUCTIONS

Some basic data for the six program stars, taken from PS00, are given in Table 1. The new observations were made with the du Pont echelle spectrograph (Shectman 1984), now outfitted with a Tektronics 2048 × 2048 CCD detector. A detailed description of the instrument and detector is provided at the Carnegie Observatories Web site.[4] The spectral resolving power was the same as employed by PS00: $R \equiv \lambda/\Delta\lambda \approx 30,000$. Each star was observed between two and four separate times, with sub-integrations combined to produce the final individual spectra.

All reductions leading to extracted, multiple-order spectra were made using standard IRAF[5] packages. The multiple exposures for each stellar spectrum were bias-subtracted and median-filtered to eliminate cosmic rays. Generally, small (<10%) sky fluxes were removed by scaling and then subtracting one of several sky observations made during each night, and the observations were divided by flat-field images. One-dimensional extractions were obtained with the IRAF *apall* task, subtracting at this time scattered light by measurement of inter-order flux. Hollow cathode Th-A comparison spectrum images, obtained before and after each stellar observation, were added and used to provide wavelength calibrations for the stellar observations.

3. RADIAL VELOCITIES

In PS00, we used a cross-correlation routine specifically designed to determine BMP radial velocities from the 2D-FRUTTI spectra. It was impractical to modify this procedure for use with the new CCD spectra. Instead, we used the IRAF *splot* routine to measure wavelengths (hence velocities) for approximately 100 lines in the wavelength range 3890–4590 Å, selected from the line list used to derive the radial velocity of our BMP cross-correlation template star, CS 22874−009. Final radial velocities were straight means of these measures to which heliocentric corrections were then applied. The individual heliocentric radial velocities are given in Table 2. Sample standard deviations calculated from measurements of 70–110 lines in individual spectra are typically 0.3 km s^{-1}. These σ-values neglect systematic effects that vary from exposure to exposure, such as non-uniform slit-illumination and spectrograph flexure. Experience has shown (see PS00, Table 4) that velocity errors derived from multiple observations of RV-constant stars are 2–4 times larger than the standard deviations for individual spectra. In Figure 1 we show individual and mean radial velocities of the RV-constant stars. The new velocities are totally consistent with those of PS00. In particular, the new RV means computed with both old and new RV measures are identical to ones just with the old RVs, and the σ-values are slightly decreased from those computed with just the older data.

The new velocities for the binary stars have been combined with those of PS00 to obtain improved orbital solutions. The derived spectroscopic orbital parameters of the Julian Date of periastron passage (JD_0), systemic velocity (V_0), velocity amplitude (K_1), eccentricity (e), longitude of periastron (ω), and period (P) are given in Table 3, along with the sample standard deviation of the orbital solution ($\sigma_{\rm orb}$), and the number of velocities used in the solution (n).

TABLE 2
NEW RADIAL VELOCITIES

Star	JD+2,450,000	RV (km s^{-1})
RV-constant Stars		
22876−042	2123.83	+42.1
22876−042	2124.84	+42.4
22941−012	2122.87	−121.6
22941−012	2123.80	−122.4
22941−012	2124.81	−122.5
22941−012	2474.83	−122.5
22964−214	2123.57	+41.3
22964−214	2124.58	+40.8
22964−214	2125.59	+41.5
Binaries		
22956−028	2123.68	+33.6
22956−028	2124.76	+33.5
22956−028	2474.68	+26.5
29497−030	2123.90	+48.3
29497−030	2124.90	+49.1
29509−027	2123.93	+77.4
29509−027	2124.93	+77.4
29509−027	2124.93	+77.4
29509−027	2474.87	+78.1

[4] See http://www.ociw.edu/lco/instruments/manuals/echelle/echelle.html.

[5] IRAF is distributed by the National Optical Astronomy Observatories, which are operated by the Association of Universities for Research in Astronomy, Inc., under cooperative agreement with the National Science Foundation.

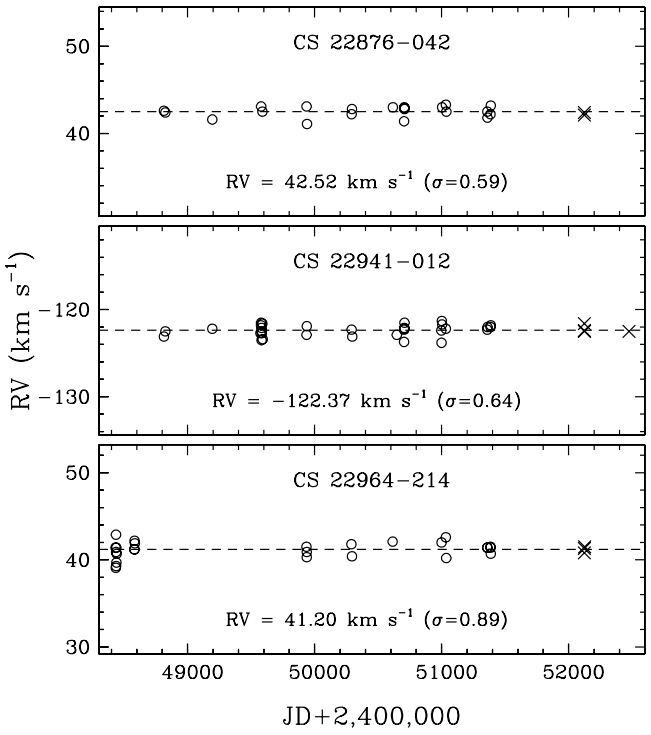

FIG. 1.—Velocities of the RV-constant stars as a function of Julian Date. The velocities from PS00 are shown as open circles, and the new velocities are shown as crosses. The vertical range in each panel of this and the next figure is 24 km s^{-1}. [*See the electronic edition of the Journal for a color version of this figure.*]

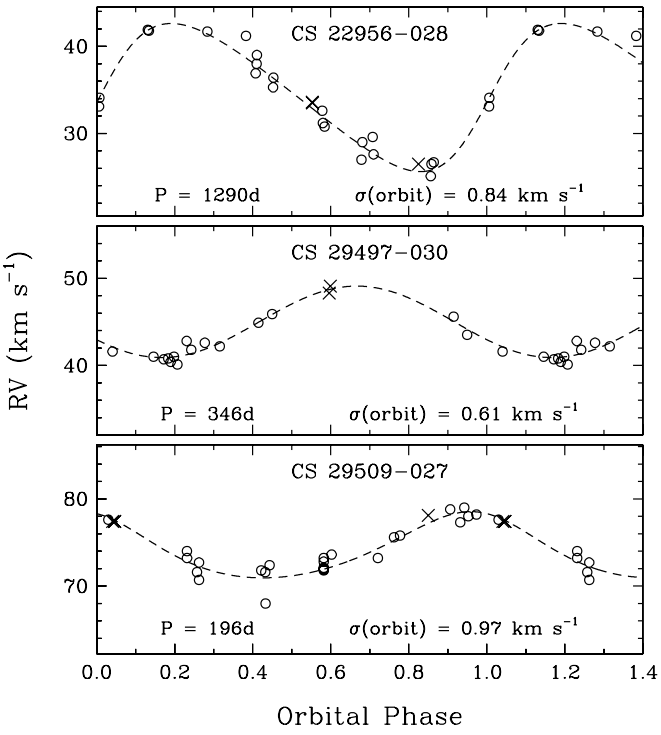

FIG. 2.—Velocities of the binary stars as a function of orbital phase. The symbols and vertical ranges of the panels are as in the previous figure. The orbital solutions, plotted as solid curves, were obtained from the parameters listed in Table 3. [*See the electronic edition of the Journal for a color version of this figure.*]

For CS 22956−028, no changes in the previous parameters were needed, but new solutions were found for CS 29497−030 and CS 29509−027. Most of the orbital parameter changes for these two stars are minor, but the newly derived eccentricities are much smaller, moving them into the long-period but nearly circular orbit category that is overrepresented among BMP binaries (see Fig. 19 of PS00). In Figure 2 the individual velocities and the derived velocity curves are plotted as functions of orbital phase.

4. ABUNDANCE ANALYSIS

As was done by PS00, we rebinned the individual spectra for each star and co-added them after shifting to a common (rest) wavelength scale. This procedure yielded S/Ns near echelle order centers for the final spectra of ∼80–100 at 6500 Å, ∼60–90 at 5000 Å, and ∼30–50 at 4000 Å. The spectra of PS00 were obtained with the 2D-FRUTTI detector that has very poor response in the yellow-red spectral region. Thus, the S/N values near 4000 Å are comparable in old and new spectra, but the S/N of the older data slowly decline with increasing wavelength to useless levels beyond the Na D lines near 5900 Å.

Inspection of the co-added new CS 29497−030 spectrum revealed the presence of CH G-band features from 4280 to 4325 Å. The combination of $T_{\rm eff} = 7050$ K and [Fe/H] = −2.16 (PS00) should render G-band lines invisibly weak if [C/Fe] ∼ 0, so a substantial overabundance of C was suggested from this detection. Additional investigation led to detection of the G band in all three of the BMP binaries but in none of the RV-constant stars. Noting also that abundances of Sr and Ba derived by PS00 were much higher in the binaries than the RV-constant stars, we undertook a new abundance analysis of C, O, and *n*-capture elements in all six BMP stars. Parameters of the atomic transitions employed in this study are given in Table 4.

The new and original spectra have comparable S/N in the blue, where the majority of lines useful for model atmosphere determination are located. Therefore, we did not repeat our previous full analysis of these stars. Table 1 lists the atmospheric parameters $T_{\rm eff}$, $\log g$, v_t, and [Fe/H] adopted from PS00, where the effective temperature is incor-

TABLE 3
ORBITAL PARAMETERS FOR THE BINARIES

Star	JD$_0$	V_0 (km s^{-1})	K_1 (km s^{-1})	e	ω	P (days)	$\sigma_{\rm orb}$ (km s^{-1})	n
22956−028.....	48831.0	+34.0	8.5	0.22	266	1290	0.97	24
29497−030.....	48500.0	+45.0	4.1	0.00	120	342	0.56	17
29509−027.....	48624.0	+74.2	3.8	0.15	20	194	0.95	29

TABLE 4
LINE DATA FOR THE ABUNDANCE ANALYSIS

Species	λ (Å)	E.P. (eV)	log *gf*	Reference
C I	5039.06	7.94	−1.79	1
C I	5052.17	7.68	−1.30	1
C I	5380.34	7.68	−1.62	1
C I	5668.94	8.53	−1.47	1
C I	6587.62	8.53	−1.00	1
C I	7111.47	8.63	−1.09	1
C I	7113.18	8.64	−0.77	1
C I	7115.18	8.63	−0.93	1
C I	7116.99	8.64	−0.91	1
O I	7771.94	9.14	+0.37	1
O I	7774.17	9.14	+0.22	1
O I	7775.39	9.14	0.00	1
Sr II	4077.71	0.00	+0.15	2
Sr II	4215.52	0.00	−0.17	2
Ba II	4554.03	0.00	+0.17	3
Ba II	5853.69	0.60	−1.01	3
Ba II	6141.73	0.70	−0.08	3
Ba II	6496.91	0.60	−0.38	3
La II	4086.71	0.00	−0.07	4
La II	4123.22	0.32	+0.13	4
Nd II	4061.09	0.47	+0.30	5
Eu II	4129.72	0.00	+0.22	6
Eu II	4205.04	0.00	+0.21	6
Pb I	4057.81	1.32	−0.17	7

REFERENCES.—(1) Wiese, Fuhr, & Deters 1996; (2) Wiese & Martin 1980; (3) Gallagher 1967; (4) Lawler, Bonvallet, & Sneden 2001; (5) Cowan et al. 2002; (6) Lawler et al. 2001; (7) Biémont et al. 2000.

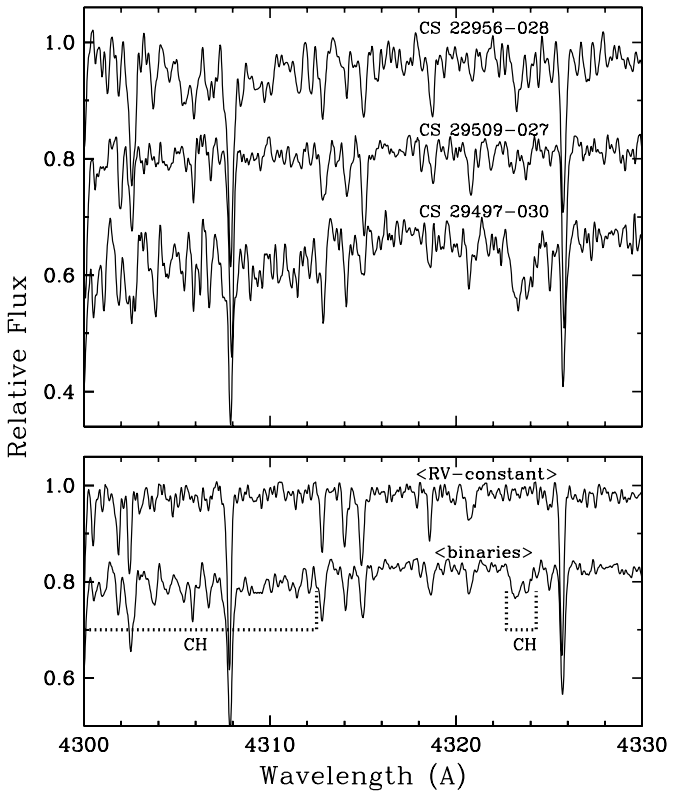

FIG. 3.—CH G band in the BMP program stars. In the upper panel, individual spectra of the three binaries are shown, and in the lower panel the mean co-added spectra of the RV-constant stars (in this and other figures labeled "RV-constant") and the binaries (labeled "binaries") are shown. In each panel the relative flux scale of the top spectrum is correct, and the other spectra are shifted downward by arbitrary additive amounts for display purposes. Regions of CH absorption are marked in the lower panel with dotted lines. [*See the electronic edition of the Journal for a color version of this figure.*]

rectly written as 7500 K; the correct value is 7050 K. To derive abundances in the present study we used model atmospheres from the Kurucz (1995)[6] grid, interpolated between grid models by software kindly provided by A. McWilliam (1990, private communication). Abundance calculations employed the current version of the LTE line analysis code MOOG (Sneden 1973).

4.1. *Carbon and Oxygen*

In the upper panel of Figure 3 we show the spectral region $4300 \leq \lambda(\text{Å}) \leq 4330$ in the three BMP binaries. CH absorption, although generally weak, can be easily detected in all three stars. The CH lines reach more than 10% depth in CS 29497−030. No CH absorption could be found in any of the RV-constant stars. To demonstrate most clearly the CH contrast between the two groups of BMP stars, we show in the lower panel of Figure 3 the averaged spectra of the RV-constant stars and the binaries. These averaged spectra were formed by simple co-additions, giving each star equal weight, after first re-binning the individual spectra and increasing the number of spectral points per spectral resolution element.

We determined C abundances for the stars from synthetic spectrum fits to their observed spectra in the wavelength range $4280 \leq \lambda(\text{Å}) \leq 4340$. The CH and atomic lines employed in these computations were culled from the Kurucz (1995) lists, as described in Rossi et al. (1999 and S. Rossi et al. 2003, in preparation). The solar photospheric abundance, employing this synthesis list, the Holweger & Müller (1974) solar model atmosphere, and the solar flux atlas of Kurucz et al. (1984), was $\log \epsilon_{\odot}(\text{C}) = 8.70 \pm 0.05$. The BMP relative abundances of C from the CH features, taken with respect to this solar abundance, are given in Table 5. They confirm that C is extremely enhanced in all three BMP binaries. Unfortunately, the upper limits on the RV-constant stars are uninformative, since they would allow undetected large C abundances in those stars as well.

Since the BMP program stars all have similar atmospheric parameters (Table 1), we also derived mean CH-based C abundances for the two groups from their averaged spectra, using the following model stellar atmospheres. For the RV-constant stars we adopted an average model with parameters ($T_{\rm eff}$, $\log g$, v_t, [Fe/H]) = (6900 K, 4.30, 2.3 km s^{-1}, −2.13), and for the binaries an average model with parameters (7000 K, 4.10, 1.9 km s^{-1}, −2.09). The mean C abundance ([C/Fe] = +1.76; Table 1) for the binaries determined from the co-added CH spectrum and the adopted mean model atmosphere is in excellent agreement with the mean of the individual abundances (fortuitously also +1.76), suggesting that this approach is valid. The mean abundance for the RV-constant stars ([C/Fe] < +0.5) is much lower than that suggested from the individual spectra (<+1.0); the increased S/N of the co-added spectrum allows a more stringent upper limit to be determined. This mean upper limit shows that

[6] See http://cfaku5.cfa.harvard.edu/.

TABLE 5

ABUNDANCES

Star	[Fe/H]	[C/Fe][a] (CH)	σ	[C/Fe] I[b]	σ	Number	[O/Fe] I	σ	Number	[Sr/Fe] II	σ	Number	[Ba/Fe] II	σ	Number
RV-constant Stars															
CS 22876−042	−2.06	<+1.0	0.3	<+1.0	0.3	2	+0.54	0.33	2	−0.29	0.10	2	−0.10	...	1
CS 22941−012	−2.03	<+1.0	0.3	<+1.0	0.3	2	+0.40	0.28	3	−0.07	0.10	2	+0.16	...	1
CS 22964−214	−2.30	<+1.0	0.3	<+1.0	0.3	2	+0.70	0.04	2	−0.20	0.25	2	−0.12	...	1
mean spectrum	−2.13	<+0.5	0.2	<+0.6	0.18	6	+0.4:	0.39	3	−0.26	0.05	2	−0.11	...	1
Binaries															
CS 22956−028	−2.08	+1.74	0.20	+1.34	0.30	3	+0.5:	0.12	2	+1.38	0.15	2	+0.37	0.26	3
CS 29497−030	−2.16	+2.17	0.10	+2.11	0.10	9	+1.13	0.09	3	+1.15	0.05	2	+2.45	0.19	4
CS 29509−027	−2.02	+1.38	0.20	+1.38	0.18	7	+0.55	0.17	3	+0.82	0.00	2	+1.33	0.13	4
mean spectrum	−2.09	+1.76	0.10	+1.54	0.22	7	+0.71	0.19	3	+1.13	0.04	2	+1.35	0.22	4

[a] Relative abundance with respect to $\log \epsilon_{\odot}(\mathrm{C}) = 8.70$, derived with our line list.

[b] Relative abundance with respect to assumed $\log \epsilon_{\odot}(\mathrm{C}) = 8.42$, derived with our line list.

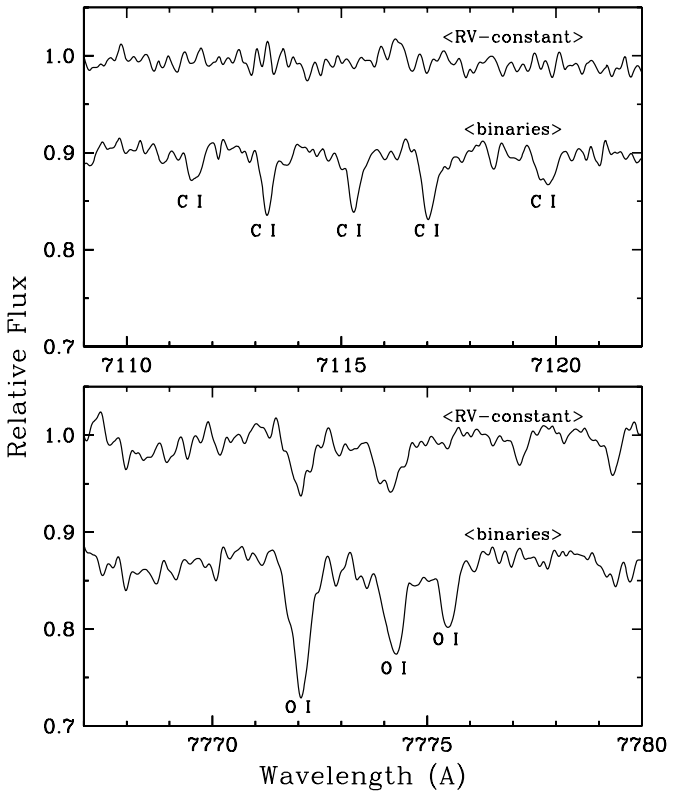

FIG. 4.—Spectra of C I and O I lines in the RV-constant and the binary BMP stars. [*See the electronic edition of the Journal for a color version of this figure.*]

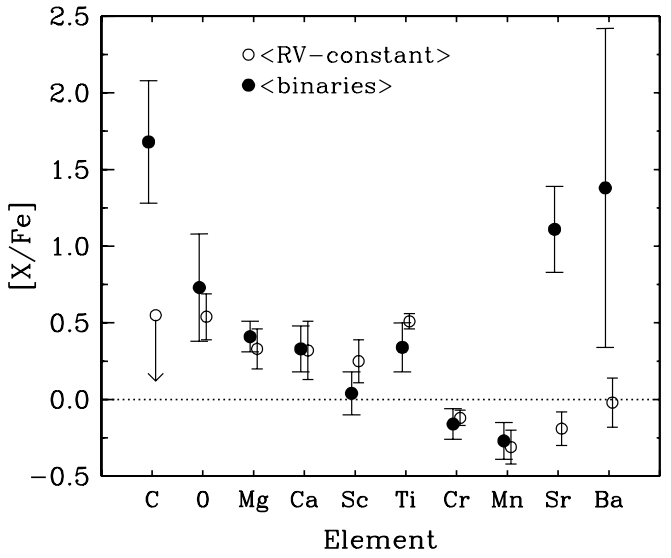

FIG. 5.—Average abundances of the BMP RV-constant and binary groups. Abundances of C, O, Sr, and Ba are from this paper, and those of the other elements are from PS00. Small horizontal shifts have been introduced to the points to the left for the binaries and to the right for the RV-constant stars, for display purposes. Each abundance and its vertical range is the mean, and the sample standard deviation σ of the values for each star in the group. The true observational/analytical uncertainties are typically about ± 0.15. Therefore, the very large ranges for C, Sr, and Ba for the binaries represent true star-to-star scatter, far beyond abundance measurement errors. [*See the electronic edition of the Journal for a color version of this figure.*]

there is no reason to suppose that C enhancements exist in the RV-constant stars.

The reality of large C enhancements in BMP binaries is strengthened by the detection of C I lines in all three of these stars. We show this in the upper panel of Figure 4 with a display of the mean spectra of RV-constant stars and binaries. As many as seven C I lines were detected on our spectra of the binaries; none of these is apparent in the RV-constant stars. Abundances and upper limits derived from these lines are listed in Table 5, again taking the differences with respect to a solar abundance of $\log \epsilon_{\odot}(\mathrm{C}) = 8.42$ derived from these same lines. Both CH and C I indicate very large overabundances, and the difference between the abundances from the two sets of features for the same BMP binary exceeds 0.2 dex only in the case of CS 22956−028, for which the C I lines are barely detectable.

The O contents of two of the BMP binaries are similar to those of the RV-constant stars. In the lower panel of Figure 4 we show the mean spectra of the two groups, indicating that the O I 7770 Å triplet lines are ∼2–3 times stronger in the binaries, but the derived O abundances (Table 5) are the same within the errors for five of the six stars. The exception is CS 29497−030, whose O abundance is ∼3–4 times larger than the other stars. This star's spectrum creates the difference in the mean O I spectra and O abundances between the two groups. The offset of CS 29497−030 appears to be real, but unfortunately no other O features are available on our spectra for confirmation.

4.2. *Strontium and Barium*

In PS00, Sr abundances were determined from the Sr II 4077, 4215 Å resonance lines, and Ba abundances from just the Ba II 4554 Å resonance line. We have repeated this analysis with the new spectra, but with the increased S/N in the yellow-red we were able to detect other strong Ba II lines at 5853, 6141, and 6496 Å. Both Sr II lines and the 4554 Å Ba II line were detected in all six stars. The abundances of Sr and Ba are listed in Table 5. The average abundances derived from the mean spectra are consistent with the means of abundances derived for each star. The new Sr and Ba values are generally consistent with those determined by PS00. The only exception is in Sr abundances of the BMP binaries, for which the new abundances are ≈0.2 dex larger in the present analysis. We attribute the difference to our use of synthetic spectrum computations in the present analysis instead of the single-line EW analysis of PS00.

It is clear that Sr and Ba generally have greater than 1 dex abundance enhancements in the BMP binaries. Since no other *n*-capture element transitions are detectable in all of the binary stars, we now illustrate the general abundance contrasts between RV-constant stars and the binaries in Figure 5. Newly derived abundances and those from PS00 are combined in this figure. Note the very good agreement for the majority of the elements in the two stellar groups. Significant differences between them occur only for C, Sr, and Ba.

4.3. *Abundances in CS 29497−030*

The C and Ba abundances of the CS 29497−030 photosphere reach or exceed their values in the Sun, in spite of this star's very low metallicity. Further examination of our new spectrum of this star revealed the presence of a few other *n*-capture transitions, most notably the 4057 Å line of Pb I. In the upper panel of Figure 6 we show the contrast in Ba II 4554 Å line strengths between CS 29497−030 and the mean

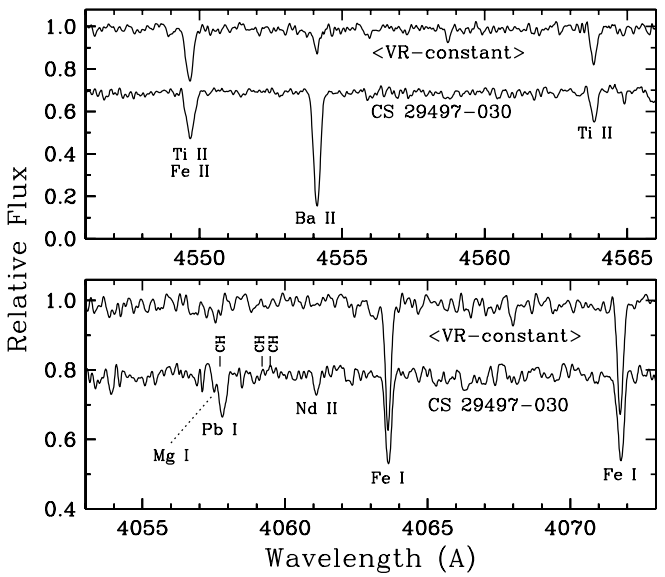

FIG. 6.—Comparison of the strongest Ba II line (*upper panel*) and the only accessible Pb I line (*lower panel*) in the mean RV-constant spectrum and in CS 294097−030. [*See the electronic edition of the Journal for a color version of this figure.*]

RV-constant star spectrum, and in the lower panel the Pb feature. Although this is the sole Pb I line available on our spectrum, the reality of the Pb absorption is not in doubt, because it can also be detected on PS00's noisier spectrum of this star.

Abundances of La, Eu, and Pb were derived from synthetic spectrum matches to the few available lines of these elements, and from the EW of the single detected Nd II line. All the CS 29497−030 abundances from this work and from PS00 are listed in Table 6. The Nd and Eu abundances should be viewed with caution. The Eu II 4129, 4205 Å lines are barely detectable on our spectra. However, the Eu abundance enhancement certainly is much less than that of Ba and probably less than those of La and Nd. The Nd II 4061 Å line should be the strongest Nd feature on our spectra, but there are other potentially useful Nd II lines (e.g., 4109.5, 4012.2 Å) that are undetectable on our spectra. Absorption is seen at Nd II 4303.6 Å, but the surrounding CH contamination prevents derivation of an Nd abundance from this feature. A spectrum of CS 29497−030 with better S/N would undoubtedly reveal the presence of many of these other lines.

TABLE 6
ABUNDANCES FOR CS 29497−030

Species	[X/Fe][a]	σ	Number
CH	+2.17	0.10	...
C I	+2.11	0.10	9
O I	+1.13	0.09	3
Mg I	+0.47	0.12	3
Ca I	+0.46	0.23	3
Sc II	+0.07	0.34	3
Ti II	+0.46	0.14	13
Cr I	−0.26	...	1
Mn I	<−0.14	...	3
Sr II	+1.15	0.05	2
Ba II	+2.45	0.19	4
La II	+1.91	0.21	2
Nd II	+2.1:	...	2
Eu II	+1.7:	0.1:	2
Pb I	+3.75	...	1

[a] Abundances of C, O, Sr, Ba, La, Nd, Eu, and Pb are from this work; the other abundances are from Paper 1.

The Pb abundance was derived taking into account the presence of a Mg I line that produces a small amount of absorption at 4057.52 Å and slightly contaminates the Pb I 4057.81 Å line. We searched for other relatively strong *n*-capture-element transitions, but they could not be detected. We also included some CH lines in our syntheses, and positions of three of the most prominent CH features are marked in the lower panel of Figure 6. The CH lines at 4059.2 and 4059.5 Å should be stronger than the potential CH contaminant to the Pb I line, but neither are detectable in our spectrum of CS 29497−030. Even with extreme relative C enhancements, the BMP binaries are too warm to produce much CH absorption in this wavelength region.

5. DISCUSSION

The very large C and *n*-capture abundances in our three very low metallicity BMP binaries, combined with $[Ba/Eu] > 0$ in at least one star, argue strongly for the creation of these anomalies by slow *n*-capture nucleosynthesis (the *s*-process) acting in He-burning (C-producing) zones of AGB stars. These enhanced abundances cannot have been synthesized in situ because of the main-sequence (i.e., pre-AGB) evolutionary state of the BMP stars. Instead, the *s*-process abundance enhancements must be the result of mass transfer from the (previous AGB) companion stars. In this section we will explore further the *s*-process in low-metallicity stars, focusing on CS 29497−030 and other Pb-rich stars, and also comment on the division between those BMP stars that have *s*-process overabundances and those that do not.

5.1. *BMP Stars and s-Process Nucleosynthesis*

The *s*-process is responsible for roughly one-half of all isotopes heavier than iron in the solar system. It has been identified as the source of *n*-capture elemental overabundances in low- and intermediate-mass (0.8–8 $M_{\odot}$) AGB stars (Busso, Gallino, & Wasserburg 1999). Previous studies have also demonstrated that the dominant source of neutrons for the *s*-process in these AGB stars is the $^{13}C(\alpha, n)^{16}O$ reaction, although some neutrons may also be produced in $^{22}Ne(\alpha, n)^{25}Mg$ reactions. As a result of convective mixing of hydrogen into the helium burning region, various concentrations of ^{13}C may be produced in these stars. Depending upon that amount of ^{13}C, relatively large neutron fluxes with respect to the iron "seed" abundance may occur. With more and more neutrons, increased enrichments of the heavier elements will occur.

For low-metallicity stars (i.e., those with $[Fe/H] \lesssim -1$) the *s*-process can lead to large overabundances of lead with respect to other *s*-process elements, such as Ba. This point is not new to our work, as other relatively Pb-rich metal-poor stars have been discovered by several groups. Most of these stars are so-called CH giants (e.g., Van Eck et al. 2001, 2003; Johnson & Bolte 2002), but an increasing number exist near the main-sequence turnoff region (e.g., Aoki et al. 2001, 2002a; Carretta et al. 2002; Lucatello et al. 2003). To

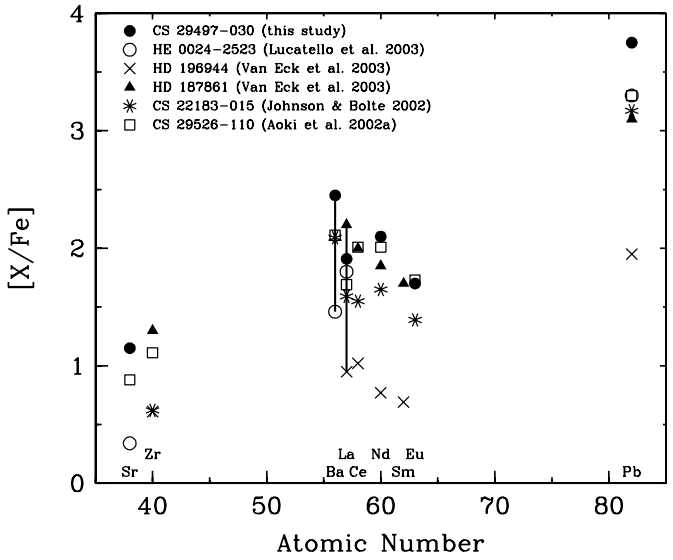

FIG. 7.—*n*-capture abundances in six extremely Pb-rich stars ([Pb/(La or Ba)] $\gtrsim +1.0$). The sources for the abundances are indicated in the figure legend. The vertical lines connecting the Ba and La abundances signify that mean abundances to be shown in the next figure have been computed after renormalization of the abundance sets from other studies to the observed Ba or La (or both) abundances of CS 29497−030. [*See the electronic edition of the Journal for a color version of this figure.*]

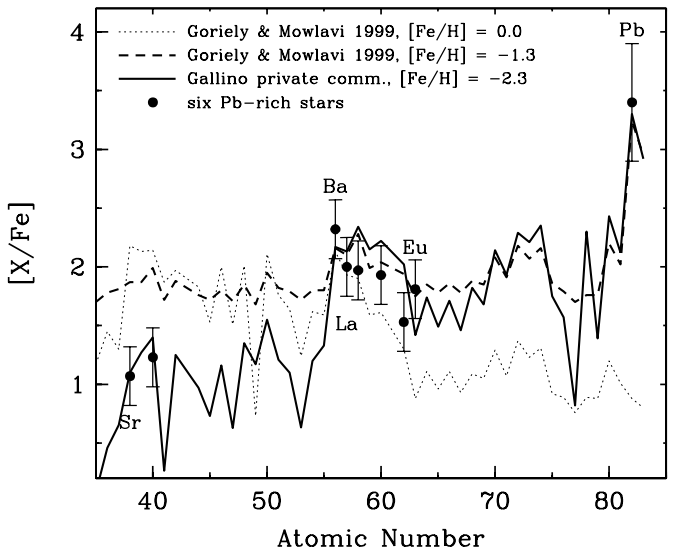

FIG. 8.—Comparison of the normalized mean *n*-capture abundances of the six Pb-rich metal-poor stars shown in the previous figure and abundance predictions of AGB star *s*-process nucleosynthesis (Goriely & Mowlavi 2000; R. Gallino 2003, private communication). Lines and symbols are defined in the figure legend. [*See the electronic edition of the Journal for a color version of this figure.*]

date, CS 29497−030 appears to be the reigning Pb abundance champion among the *s*-process–enriched metal-poor stars, both relatively ([Pb/Fe] = +3.7) and absolutely ([Pb/H] = +0.5). But it could be dethroned at any time through discovery of an even more extreme example. The Pb enhancement of CS 29497−030 also should decline when the star's convective envelope expands as it ascends the red giant branch (RGB) to become a CH giant.

A more pertinent comparison with other Pb-rich stars is in the ratio of the Pb abundance to those of lighter *n*-capture elements. In Figure 7 we display the *n*-capture abundances for six stars with the largest Pb overabundances relative to Ba or La, i.e, [Pb/(Ba or La)] $\gtrsim +1.0$. Only elements observed in at least two stars are shown in this figure. The [⟨*n*-capture⟩/Fe] values for these stars vary by more than 1 dex. In addition, different elements have been observed in different stars (in the CH giants, some elements have transitions either too strong or too blended for analysis; in the turnoff stars the lines of many element are undetectably weak). Therefore, to more easily compare results from all the studies, we have renormalized the abundances of others to agree on average with our Ba and/or La abundances in CS 29497−030. Taking all differences in the sense $\Delta[X/Fe] = [X/Fe]_{CS29497-030} - [X/Fe]_{other}$, the following offsets can be identified for the other data sets: for HE 0024−2523 (Lucatello et al. 2003), Δ[Ba/Fe] = +0.99 and Δ[La/Fe] = +0.11 for a mean of +0.55; for HD 196944 (Van Eck et al. 2003), Δ[La/Fe] = +0.96; for HD 187861 (Van Eck et al. 2003), Δ[La/Fe] = −0.29; for CS 22183−015 (Johnson & Bolte 2002), Δ[Ba/Fe] = +0.36 and Δ[La/Fe] = +0.32 for a mean of +0.34; and for CS 29526−110 (Aoki et al. 2002a), Δ[Ba/Fe] = +0.34 and Δ[La/Fe] = +0.22 for a mean of +0.28. After application of these offsets, the abundances for each element from the different studies were averaged. The star-to-star scatter of the individual normalized values for an element (other than Ba and La) was $\sigma = 0.2$–0.3 dex except for Pb, which had a wider range. Therefore, we adopted a representative scatter estimate of ±0.25 for all elements except Pb, to which we assign ±0.50.

In Figure 8 the observed mean abundances of these six Pb-rich stars are compared with theoretical *s*-process model calculations of Goriely & Mowlavi (2000) and Gallino et al. (2003; R. Gallino et al. 2003, private communication). We show Goriely & Mowlavi's *s*-process predictions arising from an initial solar metallicity abundance distribution in the *n*-capture synthesis region, and the predictions from their most metal-poor ([Fe/H] = −1.3) calculation. The Gallino et al. prediction is for an *s*-process synthesis environment with initial metallicity close to that of our BMP sample. The major neutron source in both sets of computations is assumed to be the $^{13}C(\alpha, n)^{16}O$ reaction. Vertical offsets have been applied to these three theoretical curves so that they approximately match the mean observed Ba and La abundances. The resulting agreement between the heavier ($Z \geq 56$) *n*-capture abundances and the two metal-poor *s*-process predictions are very good. The Gallino et al. distribution provides a better fit to the observed Sr and Zr abundances, but this may simply reflect the 1 dex lower metallicity of their calculation compared to that of Goriely & Mowlavi.

An important confirmation of these *s*-process nucleosynthesis arguments would be the detection of Bi in BMP binaries. This is the heaviest ($Z = 83$) *s*-process element and should also be greatly enhanced in stars such as CS 29497−030. The Bi abundance could be as large as [Bi/Pb] ~ -0.4 to -0.3 (Goriely & Mowlavi 2000; R. Gallino 2003, private communication), or $[Bi/Fe] \gtrsim +3$ in CS 29497−030 (see Fig. 8). Relatively strong Bi I lines exist in the near-UV and vacuum UV spectral regions; future observational campaigns should be able to detect these lines.

The association of large abundances of C with *s*-process production is easy to make from the connection between triple-α He-burning and the liberation of neutrons.

However, O should also be created in the same interior layers of an AGB star, from both $^{13}C(\alpha, n)^{16}O$ and more directly from $^{12}C(\alpha, \gamma)^{16}O$. Production of O is very difficult to quantify, because the reaction rate of the latter reaction is still very uncertain (e.g., Kunz et al. 2002; Heger et al. 2002; Straniero et al. 2003, and references therein). Evidence from our BMP sample is suggestive: the star with the most extreme *s*-process and C enhancements, CS 29497−030, has an O abundance 3–4 times larger than the other stars. Recently, Aoki et al. (2002b) have reported that LP 625−44, a very metal-poor subgiant with large excesses of C and the *s*-process elements, has an O overabundance that may be as much as a factor of 10 larger than HD 140283 (a star with similar $T_{\rm eff}$, $\log g$, and [Fe/H]). The discussion in that paper concentrates on O synthesis via $^{13}C(\alpha, n)^{16}O$. A large-sample comparative O abundance study between Pb-rich stars and those with more modest *s*-process overabundances could help quantitatively constrain predictions of O production in metal-poor AGB stars.

There appear to be two stellar evolutionary pathways to the *s*-process (over)production of Pb that is found in some very metal-poor main-sequence stars. CS 29497−030 is probably another example of the AGB mass-transfer paradigm (McClure & Woodsworth 1990; McClure 1997) proposed for the BMP binaries of this paper. The other path, exemplified by CS 22880−074 and CS 22898−027 (Aoki et al. 2002a), is not yet understood. The latter stars are metal-poor main-sequence stars with large C and *s*-process overabundances, but Preston & Sneden (2001) found that they exhibited no evidence of radial velocity variations from 1990 to 1999. Aoki et al. confirm the continued absence of velocity variations for both stars through 2001.

We are uncertain how to classify HE 0024−2523 into one of these groups. Its orbital period, $P = 3.41$days (Lucatello et al. 2003) lies far outside the period ranges found for both giant CH star binaries, $238 < P(\text{days}) < 2954$ (McClure & Woodsworth 1990) and subgiant CH star binaries, $878 < P(\text{days}) < 4140$ (McClure 1997). We wonder why only one of 15 CH star binaries shrank to such small orbital dimensions and can imagine two alternative explanations. In the first, the HE 0024−2523 binary is accompanied by a third star that transferred mass to both of the close binary components during its AGB evolution. The separation of this putative third star from the close pair could easily lie within the range of known CH binary system dimensions, while exceeding the minimum separation required for secular stability of a triple system, whether determined empirically (Heintz 1978) or by numerical simulation (Harrington 1977). We experimented with the published velocity data of Lucatello et al. and verified that this possibility cannot be excluded by use of the extant velocity data. We arbitrarily increased the year 2000 radial velocities by 8 km s^{-1}, a value that exceeds the largest K_1 value for McClure's subgiant CH stars, and find that we can successfully combine the altered data into a good velocity curve by making minimal adjustments to the Lucatello et al. orbital elements P, K_1, and V_0. We conclude that careful velocity measurements for several years will be required to confirm or reject the triple-star hypothesis. Batten (1973, p. 62) finds that approximately one-third of all binaries reside in triple systems, so this possibility cannot be dismissed as improbable. Finally, as a second possibility we state the obvious: HE 0024−2523 could belong to the class of *single* main-sequence stars with C and *s*-process enrichments discussed in Preston & Sneden (2001). HE 0024−2523 might just happen to have a binary companion that has nothing to do with its abundance peculiarities.

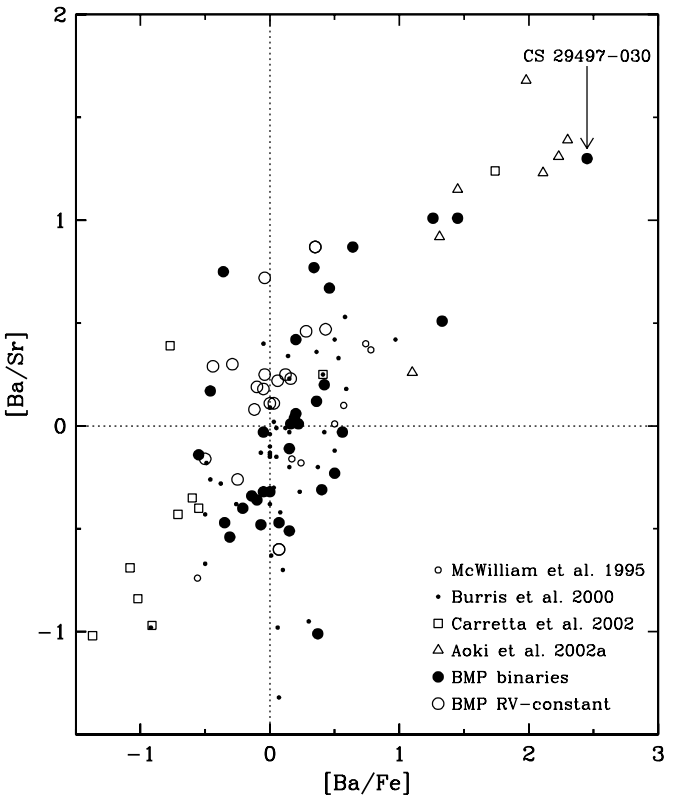

FIG. 9.—Correlation of [Ba/Sr] with [Ba/Fe] abundance ratios in metal-poor stars, combining results of several surveys. The horizontal and vertical dotted lines indicate solar ratios of [Ba/Sr] and [Ba/Fe], respectively. The abundances for BMP RV-constant stars (*large open circles*) and binaries (*large filled circles*) are taken from this study and PS00. The McWilliam et al. (1995) and Burris et al. (2000) data are included because their large sample sizes are useful in showing the domain of this diagram covered by ordinary metal-poor stars. The Carretta et al. (2002) study includes one Pb-rich star. The Aoki et al. (2002a) sample concentrated exclusively on *s*-process–rich stars. We exclude their star CS 22942−019, with its uncertain Sr abundance on the basis of extremely strong Sr II lines. [*See the electronic edition of the Journal for a color version of this figure.*]

We show in Figure 9 a comparison of the [Ba/Sr] and [Ba/Fe] ratios for a selection of metal-poor stars. These include the data sets of Aoki et al. (2002a), Carretta et al. (2002), Lucatello et al. (2003), along with our BMP binary and RV-constant stars. We have also plotted data from surveys of very metal-poor Galactic halo stars by McWilliam et al. (1995) and Burris et al. (2000). Among several interesting trends illustrated in this figure, we note that most of the stars cluster around solar values for these ratios. The Burris et al. and McWilliam et al. stars shown in the figure are dominated by the products of the rapid *n*-capture nucleosynthesis (the *r*-process), rather than the *s*-process. This is sensible since most of these metal-poor halo stars are quite old and formed prior to the main onset of Galactic *s*-process nucleosynthesis from low-mass, long stellar-evolutionary-lifetime stars. In contrast to solar material, Ba in these stars was synthesized almost entirely by the *r*-process, and thus we see relatively modest ratios of [Ba/Fe] in the surveys of McWilliam et al. and Burris et al.

In the upper right quadrant of Figure 9, several stars have exceedingly high [Ba/Fe] abundance ratios—in excess of

100 times solar. These stars show the result of extensive *s*-process enhancements of Ba. Nearly all stars with [Ba/Fe] $> +1$ have [Ba/Sr] $\gtrsim +1$. We interpret these high [Ba/Sr] ratios as a large overproduction of Ba, rather than an underproduction of Sr (see Table 7). Even more intriguing, the stars that exhibit these large [Ba/Fe] ratios include the most Pb-rich star (CS 29497−030) in our sample, the one Pb-rich metal-poor star (HE 0024−2523) from Carretta et al. and the most Pb-rich stars from the Aoki et al. study. The one-to-one correspondence between enhanced [Ba/Fe] ratios with very large Pb abundances offers convincing evidence for an abundance distribution dominated by very large enhancements of the most massive, Pb-peak, *s*-process nucleosynthesis elements. The extreme examples of *r*-process enhancement among very metal-poor stars (e.g., CS 22892−052, Sneden et al. 2003; CS 31082−001, Hill et al. 2002; BD +17°3248, Cowan et al. 2002), have $\langle$[Ba/Fe]$\rangle \approx +0.9$ but $\langle$[Ba/Sr]$\rangle \approx +0.3$. Therefore, large [Ba/Fe] ratios accompanied by very high [Ba/Sr] ratios, which can be easily estimated from the strong Ba II and Sr II resonance lines detectable in moderate-resolution spectra, offer simple observational search signatures for identifying additional Pb-rich stars.

The special case of CS 22956−028 listed in Table 5 and shown in Figure 9 deserves comment here. This star has a very large [Sr/Fe] ratio but a low [Ba/Fe] value, leading to [Ba/Sr] ≈ -1.0. We were unable to detect Pb in this star. The large [Ba/Sr] ratio in CS 22956−028 could therefore be interpreted as indicating that *s*-processing in the companion star of CS 22956−028 was much less extensive than in those cases with high Ba, and correspondingly low [Ba/Sr] values. Alternatively, Sr production might have been enhanced relative to Ba, by either the weak *s*-process (e.g., Truran et al. 2002) or perhaps even some type of primary production mechanism (e.g., Travaglio et al. 2003) in massive stars. [Ba/Sr] values $\lesssim -1.0$ are typical of *r*-process–poor stars such as HD 122563 (Truran et al.), making it unlikely that the *r*-process could be responsible for the synthesis of Sr in CS 22956−028.

5.2. *Intermediate-Age Stars versus Blue Stragglers among the Lowest Metallicity BMP stars*

We place the results presented here in the context of previous attempts to resolve BMP stars into intermediate-age and FBS subgroups (Preston et al. 1994; PS00). We restrict our attention to the 17 stars with [Fe/H] < -2 according to PS00, summarizing their properties relevant to the present discussion in Table 7. Eight of these stars possess normal or near-normal [Sr/Fe] and [Ba/Fe] values, and the mean values have small dispersion, as in the top portion of this table. These stars may actually be Sr-deficient in the mean. Tabulated upper abundance limits were not used in the calculation of means. Two of these eight stars are single-lined spectroscopic binaries, so the binary fraction for this group is 0.25, consistent with results of previous investigations of disk (Duquennoy & Mayor 1991) and halo (Latham et al. 1998) main-sequence binary frequency. If we include the very metal-poor double-lined spectroscopic binary CS

TABLE 7
SUMMARY PROPERTIES OF LOWEST METALLICITY BMP STARS

Star	Class[a]	$v \sin i$[b] (km s^{-1})	[Fe/H][c]	[Sr/Fe][c]	[Ba/Fe][c]	P[d] (days)	$a \sin i/R_\odot$
			Intermediate Age				
CS 22873−139	SB	10	−2.85	...	...	19	9
CS 22876−042	RVC	8	−2.06	−0.29	−0.10	...	...
CS 22880−013	RVC	12	−2.05	−0.59	<−0.29	...	...
CS 22941−005	SB	25	−2.43	−0.43	<+0.34	3243000	42382
CS 22941−012	RVC	10	−2.03	−0.07	+0.16	...	...
CS 22950−173	RVC	8	−2.50	−0.76	−0.04	...	...
CS 22960−058	RVC	10	−2.13	−0.13	+0.12	...	...
CS 22964−214	RVC	12	−2.30	−0.20	−0.12	...	...
CS 29499−057	SB	25	−2.33	−0.23	<+0.64	2500	92
Mean				−0.34	0.00		
σ				0.24	0.13		
			Field Blue Straggler				
CS 22890−069	SB	80	−2.00	...	...	2	1.3
CS 22946−011	SB	15	−2.59	+0.25	+1.26	585	126
CS 22956−028	SB	15	−2.08	+1.38	+0.37	1290	210
CS 22963−013	SB	70	−2.50	...	...	85	21
CS 29497−030	SB	12	−2.16	+1.15	+2.45	342	25
CS 29509−027	SB	10	−2.01	+0.82	+1.33	194	14
CS 29518−039	SB	17	−2.49	+0.44	+1.45	1630	254
CS 29527−045	SB	35	−2.14	−0.34	...	84	27
Mean				+0.62	+1.37		
σ				0.63	0.74		

[a] RVC = RV-constant star; SB = spectroscopic binary.
[b] PS00, Table 1.
[c] This paper, Table 5, otherwise PS00, Table 7; for CS 22890−069 and CS 22963−013 [Fe/H] estimates from K-line strength are from PS00, Table 1.
[d] This paper, Table 3, otherwise PS00, Table 5.

22873−139 (Preston 1994; Thorburn 1994), the binary fraction rises to 0.33, somewhat large but uncertain because of the small database. We suggest that these nine stars are intermediate-age metal-poor main-sequence stars.

The remaining eight stars, listed in the bottom portion of Table 7, are all spectroscopic binaries. The [Sr/Fe] and [Ba/Fe] values for five of them are significantly higher than solar, and their means exceed those of the upper portion of Table 7 by an order of magnitude or more, thus conforming to our view that the abundance peculiarities of this group arise from mass transfer during AGB evolution of their companions. Three additional binaries, also listed in the bottom portion of Table 7, exhibit large rotational line-broadening ($v \sin i \geq 35$ km s^{-1}) that precluded nearly all measurements of Sr and Ba lines in our rather noisy spectra, so we can say nothing about the element-to-Fe ratios. In view of their relatively short orbital periods, we regard it likely that they experienced RGB rather than AGB mass transfer, if they are in fact post-mass transfer binaries. The very low [Sr/Fe] value of CS 29527−045 supports, but cannot prove, this suspicion. We identify these eight binary BMP stars as bona fide FBS analogs. If these assignments are correct, the FBS fraction of the most metal-poor BMP stars is $8/17 = 0.47$, a modest 20% smaller than the value 0.6 estimated by PS00. Thus, the most metal-poor BMP stars are not unusual with regard to their makeup. Note that were we to assign the three rapid rotators to the intermediate age group, the FBS fraction would fall to $5/17 = 0.29$, and the intermediate-age component would become uncomfortably large (e.g., see Unavane, Wyse, & Gilmore 1996).

It is surprising that all five of the FBSs with [Fe/H] < -2 for which we can measure both Sr and Ba abundances exhibit *s*-process enrichment. The orbital periods of these five stars, which lie in the range $196 \leq P(\text{days}) \leq 1630$, and the $a \sin i$ values derived from them in the last column of Table 7 appear to be drawn at random from those of the 42 binaries studied by PS00. None of the more metal-rich BMP binaries show significant *s*-process enrichment, but, as noted by our referee, a steep dependence of C and *s*-process enrichment on [Fe/H] may simply be an indication that the accreted mass fractions of these elements are approximately independent of metallicity, as illustrated by the calculations presented in Figure 11 of Smith, Coleman, & Lambert (1993). Therefore, additional AGB mass transfer binaries may be present but undetected among the more metal-rich BMP binary sample. About half of the BMP binaries with [Fe/H] < -2 avoided mass transfer during RGB evolution (see PS00, the [Ba/Fe] panel of Fig. 17), so we can only suppose that their large initial orbital dimensions precluded Roche lobe overflow, and that their orbits shrank during subsequent AGB evolution, when Roche lobe overflow must have occurred to provide the observed abundance anomalies and elevated main-sequence locations of these stars. We argue the case for Roche lobe overflow rather than accretion in an AGB superwind, because Theuns et al. (1996) find that wind accretion transfers no more than 2%–3% of the wind mass from the donor to the receiver, an amount insufficient to move even the most massive MS (turnoff) stars to their FBS positions above the main-sequence turnoff. Furthermore, the effect of nonconservative mass loss by the wind is to *increase* both the semimajor axis and the period, not to reduce them. Fortunately, a substantial number of additional BMP candidates are available (Preston et al. 1994) for further investigation of this intriguing puzzle.

Finally, the classification scheme in Table 7 can be subjected to the lithium test. Metal-poor intermediate-age stars should lie on the Spite plateau (Spite & Spite 1982; Thorburn 1994), while lithium abundances in the surface layers of FBSs should be greatly diminished because of destruction of lithium in the red giant envelopes of their companions, as discussed, for example, by PS00 and Ryan et al. (2001).

6. SUMMARY

Our observations have indicated that there are distinct differences in the abundances of BMP binaries and RV-constant stars. The binaries are rich in C and *n*-capture elements. We also suspect that this class of objects is rich in O and, if so, might provide interesting constraints on the poorly known, but very critical, $^{12}C(\alpha, \gamma)^{16}O$ reaction. We have argued that most likely mass transfer from the former AGB companion star produced the *n*-capture element abundances now observed in the BMP binary stars. We have further found that the *n*-capture element abundances show the clear signature of the *s*-process, and in particular show enhancements of the heaviest, Pb-peak, such elements. Our observations have demonstrated that very large values of [Ba/Fe], with correspondingly large values of [Sr/Ba], are associated directly with Pb-rich stars. One of these stars, CS 29497−030, has the largest Pb abundance of any star yet observed. This would further imply that Bi abundances should be high in this star, but we have not yet been able to confirm that. Finally, we have drawn attention again to the class distinction between the BMP binaries, which we identify as true field blue stragglers, and BMP RV-constant stars, which we again suggest are intermediate-age stars probably accreted by our Galaxy from nearby satellite dwarf spheroidals.

BMP binary stars are not alone in exhibiting C and *s*-process enhancements, nor are they unique in the suggested links between binary membership, AGB-created abundance anomalies, and mass transfer. However, these objects represent the first stellar class for which this particular evolutionary scenario may be "complete." BMP binaries are misfits in the metal-poor HR diagram that, together with the abundance information presented here, clearly indicates their acquisition in the past of substantial amounts of envelope material from their companion stars. Obviously further studies of these very interesting objects are warranted and will be needed to help fill in remaining parts of the story.

We thank David Lambert, Peter Höflich, Craig Wheeler, and the referee for helpful discussions and suggestions for improvements to this paper. Portions of this study were completed while C. S. was a Visiting Scientist at the Carnegie Observatories; their hospitality and financial support are gratefully acknowledged. This research has been supported in part by NSF grants AST-9987162 to C. S. and AST-9986974 to J. J. C.

REFERENCES

Aoki, W., Ryan, S. G., Norris, J. E., Beers, T. C., Ando, H., Iwamoto, N., Kajino, T., Mathews, G. J., & Fujimoto, M. Y. 2001, ApJ, 561, 346
Aoki, W., Ryan, S. G., Norris, J. E., Beers, T. C., Ando, H., & Tsangarides, S. 2002a, ApJ, 580, 1149
Aoki, W., et al. 2002b, PASJ, 54, 427
Batten, A. 1973, Binary and Multiple Systems of Stars (Oxford: Pergamon)
Biémont, E., Garnir, H. P., Palmeri, P., Li, Z. S., & Svanberg, S. 2000, MNRAS, 312, 116
Burris, D. L., Pilachowski, C. A., Armandroff, T. A., Sneden, C., Cowan, J. J., & Roe, H. 2000, ApJ, 544, 302
Busso, M., Gallino, R., & Wasserburg, G. J. 1999, ARA&A, 37, 239
Carretta, E., Gratton, R., Cohen, J. G., Beers, T. C., & Christlieb, N. 2002, AJ, 124, 481
Cowan, J. J., et al. 2002, ApJ, 572, 861
Duquennoy, A., & Mayor, M. 1991, A&A, 248, 485
Gallagher, A. 1967, Phys. Rev., 157, 24
Gallino, R., et al. 2003, Nucl. Phys. A, 718, 181
Goriely, S., & Mowlavi, N. 2000, A&A, 362, 599
Harrington, R. S. 1977, Rev. Mexicana Astron. Astrofis., 3, 139
Heger, A., Woosley, S. E., Rauscher, T., Hoffman, R. D., & Boyes, M. M. 2002, NewA Rev., 46, 463
Heintz, W. D. 1978, Double Stars, Geophysics, and Astrophysics Monographs, Vol. 15 (Dordrecht: Reidel), 66
Hill, V., et al. 2002, A&A, 387, 560
Holweger, H., & Müller, E. A. 1974, Sol. Phys., 39, 19
Johnson, J. A., & Bolte, M. 2002, ApJ, 579, L87
Kunz, R., Fey, M., Jaeger, M., Mayer, A., Hammer, J. W., Staudt, G., Harissopulos, S., & Paradellis, T. 2002, ApJ, 567, 643
Kurucz, R. L. 1995, in ASP Conf. Ser. 81, Workshop on Laboratory and Astronomical High-Resolution Spectra, ed. A. J. Sauval, R. Blomme, & N. Grevesse (San Francisco: ASP), 583
Kurucz, R. L., Furenlid, I., Brault, J., & Testerman, L. 1984, Solar Flux Atlas from 296 to 1300 nm (Cambridge: Harvard)
Latham, D. W., Stefanik, R. P., Mazeh, T., Goldberg, D., Torres, G., & Carney, B. W. 1998, in ASP Conf. Ser. 154, Cool Stars, Stellar Systems, and the Sun, ed. R. A. Donahue & J. A. Bookbinder (San Francisco: ASP), 2129
Lawler, J. E., Bonvallet, G., & Sneden, C. 2001, ApJ, 556, 452
Lawler, J. E., Wickliffe, M. E., den Hartog, E. A., & Sneden, C. 2001, ApJ, 563, 1075
Lucatello, S., Gratton, R., Cohen, J. G., Beers, T. C., Christlieb, N., Carretta, E., & Ramirez, S. 2003, AJ, 125, 875
McClure, R. D. 1997, PASP, 109, 536
McClure, R. D., & Woodsworth, A. W. 1990, ApJ, 352, 709
McCrea, W. H. 1964, MNRAS, 128, 147
McWilliam, A., Preston, G. W., Sneden, C., & Searle, L. 1995, AJ, 109, 2757
Preston, G. W. 1994, AJ, 108, 2267
Preston, G. W., Beers, T. C., & Shectman, S. A. 1994, AJ, 108, 538
Preston, G. W., & Sneden, C. 2000, AJ, 120, 1014 (PS00)
———. 2001, AJ, 122, 1545
Rossi, S., Beers, T. C., & Sneden, C. 1999, in ASP Conf. Ser. 165, The Third Stromlo Symposium: the Galactic Halo, ed. B. K. Gibson, T. S. Axelrod, M. E. Putman (San Francisco: ASP), 264
Ryan, S. G., Beers, T. C., Kajino, T., Rosolankova, K. 2001, ApJ, 547, 231
Shectman, S. A. 1984, Proc. SPIE, 445, 128
Sills, A., & Bailyn, C. D. 1999, ApJ, 513, 428
Smecker-Hane, T., Stetson, P., B., Hesser, J. E., & Lennert, M. D. 1994, AJ, 108, 507
Smith, V. V., Coleman, H., & Lambert, D. L. 1993, ApJ, 417, 287
Sneden, C. 1973, ApJ, 184, 839
Sneden, C., et al. 2003, ApJ, in press
Spite, F., & Spite, M. 1982, A&A, 115, 357
Straniero, O., Domínguez, I., Imbriani, G., & Piersanti, L. 2003, ApJ, 583, 878
Stryker, L. L. 1993, PASP, 105, 1081
Theuns, T., Boffin, H. M., & Jorissen, A. 1996, MNRAS, 280, 1264
Thorburn, J. A. 1994, ApJ, 421, 318
Travaglio, C., Gallino, R., Cowan, J. J., Jordan, F., & Sneden, C. 2003, ApJ, submitted
Truran, J. W., Cowan, J. J., Pilachowski, C. A., & Sneden, C. 2002, PASP, 114, 1293
Unavane, M., Wyse, R. F. G., & Gilmore, G. 1996, MNRAS, 278, 727
Van Eck, S., Goriely, S., Jorissen, A., & Plez, B. 2001, Nature, 412, 793
———. 2003, preprint (astro-ph/0302075)
Vilhu, O. 1982, A&A, 109, 17
Wiese, W. L., Fuhr, J. R., & Deters, T. M. 1996, Atomic Transition Probabilities of Carbon, Nitrogen, and Oxygen: A Critical Data Compilation (Washington, DC: Am. Chem. Soc.)
Wiese, W. L., & Martin, G. A. 1980, Wavelengths and Transition Probabilities for Atoms and Atomic Ions: Part II, NBS-NSRDS No. 68 (Washington: GPO)